



# Massive black hole binaries in gaseous nuclear discs

M. Dotti<sup>1</sup>, M. Colpi<sup>2</sup>, F. Haardt<sup>3</sup>, and L. Mayer<sup>4,5</sup>

<sup>1</sup> Department of Astronomy, University of Michigan, Ann Arbor, MI 48109, USA  
e-mail: mdotti@umich.edu

<sup>2</sup> Dipartimento di Fisica G. Occhialini, Università degli Studi di Milano Bicocca, Piazza della Scienza 3, 20126 Milano, Italy

<sup>3</sup> Dipartimento di Fisica e Matematica, Università dell'Insubria, Via Valleggio 11, 22100 Como, Italy

<sup>4</sup> Institute for Theoretical Physics, University of Zurich, CH-8057, Zurich, Switzerland

<sup>5</sup> Institute of Astronomy, Department of Physics, ETH, Zurich, Wolfgang-Pauli Strasse, CH-8095 Zurich, Switzerland

**Abstract.** We study the evolution of a massive black hole pair in a rotationally supported nuclear disc. The distributions of stars and gas mimic the nuclear region of a gas-rich galaxy merger remnant. Using high-resolution SPH simulations, we follow the black hole dynamics and trace the evolution of the underlying background, until the black holes form a binary. We find that the gravitational perturbation of the pair creates a core in the disc density profile, hence decreasing the gas-dynamical drag. This leads the newly formed binary to stall at a separation of  $\sim 5$  pc. In the early phases of the sinking, black holes lose memory of their initial orbital eccentricity if they co-rotate with the disc, as rotation of the gaseous background promotes circularization of the BH orbits. Circularization is efficient until the black holes bind in a binary, though in the latest stages of the simulations a residual eccentricity  $\gtrsim 0.1$  is still present. Black holes are treated as sink particles, allowing for gas accretion. We find that accretion strongly depends on the dynamical properties of the black holes, and occurs preferentially after circularization.

**Key words.** Black hole physics – Hydrodynamics – Galaxies: starburst – Galaxies: evolution – Galaxies: nuclei

## 1. Introduction

Collisions of gas rich spiral galaxies may trigger starbursts as those observed in luminous infrared galaxies (LIRGs). A large number of LIRGs hosts a central rotationally supported massive (up to  $10^{10}M_{\odot}$ ) gaseous disc extending on scales of  $\sim 100$  pc (Sanders & Mirabel 1996; Downes & Solomon 1998). These discs may be the end-product of

gas-dynamical, gravitational torques excited during the merger, when large amounts of gas is driven into the core of the remnant (Kazantzidis et al. 2005; Mayer et al. 2007).

Inside a massive self-gravitating disc, a putative MBH pair can continue its dynamical evolution, and, possibly, can accrete gas, producing an observable double AGN (Kocsis et al. 2005, Dotti et al. 2006). Here we study the role of a nuclear gaseous disc in driving the or-

bital evolution of the MBH binary, and assesses the possibility of gas accretion into each pair member.

## 2. Simulation setup

We follow the dynamics of MBH pairs in nuclear discs using numerical simulations run with the N-Body/SPH code GADGET (Springel, Yoshida & White 2001).

In our models, two MBHs are placed in the plane of a gaseous disc, embedded in a larger scale stellar spheroid. The gaseous disc is modeled with  $2 \times 10^6$  particles, has a total mass  $M_{\text{Disc}} = 10^8 M_{\odot}$ , and follows a Mestel surface density profile. The disc is rotationally supported, and has a radial and vertical scale of 100 and 10 pc, respectively. SPH particles evolve adiabatically (with a polytropic index = 5/3), and we set the initial internal energy density profile so that the Toomre parameter of the disc is  $> 3$  everywhere, preventing disc fragmentation and formation of large scale over-densities, such as bars and spiral arms.

The spheroidal component (bulge) is modeled with  $10^5$  collisionless particles, initially distributed as a Plummer sphere, with a core radius of 50 pc, and a total mass  $M_{\text{Bulge}} = 6.98 M_{\text{Disc}}$ .

The two MBHs are equal mass ( $M_{\text{BH}} = 4 \times 10^6 M_{\odot}$ ).  $M_1$  is placed at rest at the centre of the circumnuclear disc, while  $M_2$  is initially orbiting in the plane of the disc on an orbit whose eccentricity is  $\approx 0.7$ , at a separation of 50 pc from  $M_1$ .  $M_2$  can either be co- or counter-rotating with respect to the circumnuclear disc (runs A and B, respectively).

We allow the gas particles to be accreted onto the MBHs if the two following criteria are fulfilled:

- the total energy (kinetic + internal + gravitational) of the gas particle is lower than 7/10 of its gravitational energy (all the energies are computed with respect to each MBH)
- the total mass accreted onto a MBH every timestep is lower than the  $\dot{M}$  corresponding to an Eddington luminosity ( $L_{\text{Edd}}$ ) assuming a radiative efficiency of 10%.

The spatial resolution of the hydrodynamical force in the highest density regions is  $\approx 0.1$

pc. We set the gravitational softening for the gaseous particles and the MBHs at the same value to prevent numerical errors due to the different resolution. With this spatial resolution we can resolve the influence radius of  $M_1$  ( $\approx 1$  pc), a condition necessary to assess gas accretion<sup>1</sup>.

## 3. MBHs dynamical evolution

The upper panel of Fig. 1 shows the separation between the two MBHs as a function of time for run A. The two MBHs reach a separation of the order of few pc in less than 10 Myr. After an initial fast migration, the shrinking process becomes inefficient and the binary stalls at a separation of  $\approx 5$  pc, larger than our force resolution.

The eccentricity evolution of the MBH pair is presented in the middle panel of Fig. 1. The MBH pair loses memory of its initial eccentricity in the early phases of the orbital decay, when the two MBH are at a separation of  $\sim 10$  pc. Such circularization happens because of the different effects that dynamical friction exerts on  $M_2$  at different orbital phases (see Dotti, Colpi & Haardt 2006; Dotti et al. 2007 for a detailed review). Dynamical friction is efficient in reducing the eccentricity down to values  $< 0.1$ , while, when the binary forms, eccentricity grows again, up to  $\approx 0.1$ .

The stalling of the MBH pair and the residual eccentricity are due to the formation of a central core in the gaseous disc, as shown in Fig. 2. The primary cause of the core formation is energy and angular momentum transfer from the orbiting MBH to the disc due to the dynamical friction. The inner core forms during the early phases of the MBH orbital decay, when  $M_2$  orbit is still eccentric. We note that the interaction between the MBHs and the circumnuclear disc in this phase was not fully resolved in Dotti et al. (2007). As a check of our initial conditions, we evolved the disc without  $M_2$  for  $\sim 10^7$  yr, and no core formation was observed. We also ran the same simulation with accretion switched off, and we found no differ-

<sup>1</sup> The influence radius of  $M_2$  depends on the phase of its orbit.

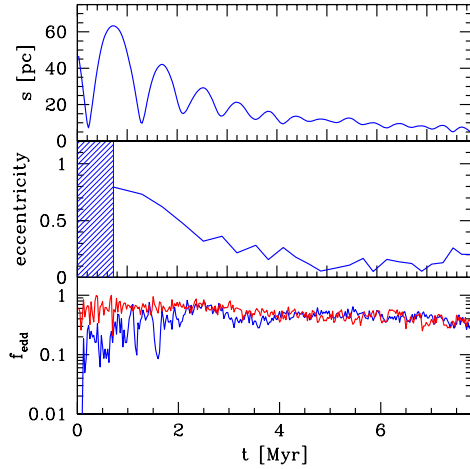


**Fig. 1.** Run A. Upper panel: MBH separation as a function of time. Middle panel: MBH pair eccentricity evolution. The shaded area refers to the time before the first apocentre, when we can not evaluate the value of the eccentricity. Lower panel: Eddington accretion ratio as a function of time. Red and blue lines refer to M1 and M2, respectively.

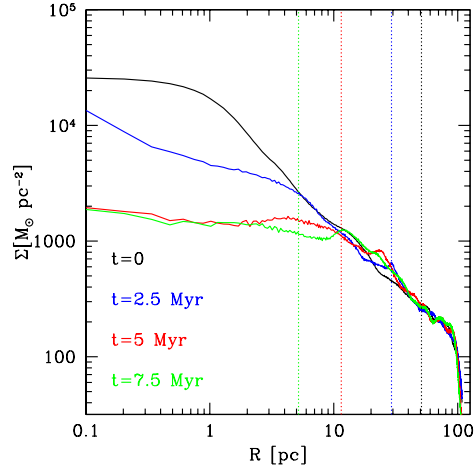


**Fig. 2.** Surface density profile of the circumnuclear disc at four different times in run A. The solid black, blue, red and green solid lines refer to  $t = 0, 2.5, 5,$  and  $7.5$  Myr respectively. The vertical dotted lines refer to the current position of  $M_2$  at the four times.

ences in the dynamical evolution of the MBH pair, as expected due to the small amount of gas accreted by the MBHs with respect to the total mass of the circumnuclear disc ( $\sim 0.1\%$ ).

For the counter-rotating case (Run B) we find that the two MBHs also stall at a separation of  $\approx 5$  pc with a non zero eccentricity as illustrated in Fig. 3. The middle panel of Fig. 3 shows the evolution of the  $z$ -component of the orbital angular momentum  $L_z$  of  $M_2$ , normalized to its initial value. The angular momentum (initially negative) grows very efficiently during the first Myr, when  $M_2$  is passing through the central, high density region of the disc. Angular momentum continues to grow monotonically for the next 3–4 Myrs, then becomes positive ( $L_z \approx 0.1$ ). That is,  $M_2$  starts to move on a co-rotating orbit with respect to the disc. The dynamical friction process is the ultimate cause of this orbital “angular momentum flip”.

#### 4. Accretion processes

Fig. 1 and 3 allow a direct comparison between the dynamical properties of the two MBHs and

the accretion rates in runs A and B respectively. The upper panels show the MBHs separation, while the lower panels show the Eddington ratio  $f_{\text{Edd}} \equiv \dot{M}/\dot{M}_{\text{Edd}}$  for the central (red lines) and orbiting (blue lines) MBHs. In both runs,  $M_1$  accretes at  $f_{\text{Edd}} \approx 0.5$ , with a slight decrease with time.  $M_2$ , instead, behaves differently. In run A, during the first 7 Myrs, on average it owns  $f_{\text{Edd}} \approx 0.4$ .  $M_2$  accretion history can be divided in two phases:

1a) for  $t \lesssim 2.5$  Myrs the circularization process is still efficient. During this phase  $f_{\text{Edd}} \approx 0.3$  on average, showing strong variability;  
 2a) for  $t \gtrsim 2.5$  Myrs,  $M_2$  is moving on a quasi-circular orbit, and the relative velocity between  $M_2$  and the gaseous disc is reduced. In this phase,  $f_{\text{Edd}} \approx 0.45$  on average.

Larger variability of  $f_{\text{Edd}}$  can be observed onto the counter-rotating  $M_2$  in run B. We can still distinguish two phases: 1b) for  $t \lesssim 3$  Myr,  $M_2$  is still counter-rotating ( $L_z < 0$ ), and  $f_{\text{Edd}} \approx 0.1$ , well below  $f_{\text{Edd}} \approx 0.25$  obtained averaging over 5 Myr;

2b) for  $t \gtrsim 3$  Myr,  $M_2$  accretes at  $f_{\text{Edd}} \approx 0.45$  (on average).

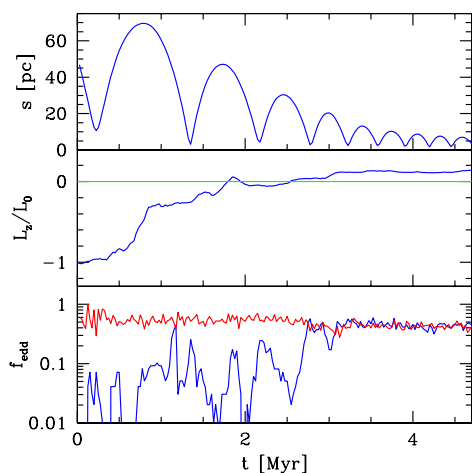


**Fig. 3.** Run B. Upper panel: MBHs separation as a function of time. Lower panel: Eddington accretion ratio as a function of time. Red and blue lines refer to  $M_1$  and  $M_2$ , respectively.

## 5. Conclusions

Our two high resolution runs show that the gas–dynamical interaction between the massive circumnuclear disc and MBHs is unable to bring the two MBHs at separations of the order of the force resolution ( $\approx 0.1$  pc) in  $\approx 5$  Myr. Circularization of the initially eccentric orbit of  $M_2$  is efficient until the MBHs form a binary. In the latest stages of our simulations 1 eccentricity grows again up to  $\gtrsim 0.1$ . These results are strictly connected to the formation of a central core in the surface density profile of the circumnuclear disc, due to the energy and angular momentum exchange between the MBH pair and the gaseous particles. We stress that we could catch the formation of the central core (and the stalling of the binary) because of the high spatial resolu-

tion adopted from the beginning of the simulation, which was increased by a factor  $\approx 10$  compared to our previous simulations. It must be pointed out that, as discussed in Mayer et al. 2007, the fate of the MBH binary could be strongly affected by cooling/heating processes, not implemented in our runs.

Thanks to the high spatial resolution of our simulations that allows for the code to resolve the sphere of influence of the MBHs, we studied for the first time the mass accretion rate as a function of the dynamical properties of the MBHs: we found that variable double nuclear activity can be observable for few Myr, when the two MBHs orbit with relative separations  $\approx 10$  pc. The accretion rate on counter–rotating orbits is more variable, and lower by a factor of 4–5 when compared to  $M_2$  co–rotating with the disc.

## References

- Dotti M., Colpi M., Haardt F., 2006, MNRAS, 367, 103
- Dotti M., Salvaterra R., Sesana A., Colpi M., Haardt F., 2006, MNRAS, 372, 869
- Dotti M., Colpi M., Haardt F., Mayer L., 2007, MNRAS, 379, 956
- Downes D., Solomon P.M., 1998, ApJ, 507, 615
- Kazantzidis S. et al., 2005, ApJ, 623, L67
- Kocsis B., Frei Z., Haiman Z., Menou K., 2005, ApJ, 637, 27
- Mayer L., Kazantzidis S., Madau P., Colpi M., Quinn T., Wadsley J., 2007, Science, 316, 1874
- Sanders D.B., Mirabel I.F., 1996, ARA&A, 34, 749
- Springel V., Yoshida N., White S.D.M., 2001, NewA, 6, 79